

NGU Report 2013.049

Helicopter-borne magnetic and radiometric  
geophysical survey at Kviteseid, Notodden,  
Ulefoss, in Telemark county.

Report no.: 2013.049		ISSN 0800-3416	Grading: Open
Title: Helicopter-borne magnetic and radiometric geophysical at Kviteseid, Notodden, Ulefoss in Telemark county Nordland.			
Authors: Alexandros Stampolidis, Frode Ofstad and Vikas Baranwal		Client: NGU	
County: Telemark		Municipalities: Andebu, Hof, Hole, Holmestrand, Kongsberg, Krødsherad, Lardal, Modum, Ringerike, Sigdal, Skien, Siljan, Våle og Øvre Eiker	
Map-sheet name (M=1:250.000) Skien		Map-sheet no. and -name (M=1:50.000) 1613 I Bø, 1613 IV Seljord, 1614 II Gransherad, 1614 III Hjartdal, 1713 IV Nordagutu, 1714 III Notodden	
Deposit name and grid-reference: Notodden WGS 84, UTM zone 32V, 515000 E, 6602500 N		Number of pages: 28 Price (NOK): Map enclosures:	
Fieldwork carried out: June-July 2013 (land) 18 Oct 2013 (lakes)	Date of report: March 12 <sup>th</sup> 2014	Project no.: 327600	Person responsible: <i>Jan S. Rønning</i>
<p>Summary:</p> <p>NGU conducted an airborne magnetic and radiometric survey over the Kviteseid, Notodden and Ulefoss regions, in Telemark county between June-July 2013 as a part of the MINS project (Mineral resources in South Norway). At a second phase of this survey the lakes of Norsjo and Seljordsvatn were measured on 18<sup>th</sup> of October of the same year. This report describes and documents the acquisition, processing and visualization of recorded datasets. The geophysical survey results reported herein are approximately 9960 line km, covering an area of approximately 1960 km<sup>2</sup>.</p> <p>Two helicopter-borne systems were used in this survey. More than 95% of the total flights were conducted at the first phase of the acquisition period with a helicopter-borne system that was designed to obtain detailed airborne magnetic and radiometric data. It had a Scintrex Cs-3 magnetometer in a towed bird and a 1024 channels RSX-5 spectrometer installed under the helicopter belly. The helicopter-borne system that flown over the lakes of Norsjo and Seljordsvatn, had a Scintrex Cs-2 for the magnetic field recordings and a similar 1024 channels RSX-5 spectrometer installed under the helicopter for gamma-rays.</p> <p>The entire survey was flown with 200 m line spacing. The flight line direction was 140° (NW-SE). The average speed ranged daily between 60 and 90 km/h, depending mainly on the local topography. The average terrain clearance of the helicopter was about 80 m.</p> <p>Collected data were processed at NGU using Geosoft Oasis Montaj software. Raw total magnetic field data were corrected for diurnal variations and levelled using standard micro-levelling algorithm. Radiometric data were processed using standard procedures recommended by International Atomic Energy Association.</p> <p>Data were gridded with a cell size of 50 x 50 m and presented as shaded relief maps at the scale of 1:75.000.</p>			
Keywords:	Geophysics	Airborne	
Magnetic	Radiometric	Technical report	

## Table of Contents

<b>1.</b>	<b>INTRODUCTION</b> .....	<b>5</b>
<b>2.</b>	<b>SURVEY SPECIFICATIONS</b> .....	<b>6</b>
<b>2.1</b>	<b>Airborne Survey Parameters</b> .....	<b>6</b>
<b>2.2</b>	<b>Airborne Survey Instrumentation</b> .....	<b>9</b>
<b>2.3</b>	<b>Airborne Survey Logistics Summary</b> .....	<b>9</b>
<b>3.</b>	<b>DATA PROCESSING AND PRESENTATION</b> .....	<b>11</b>
<b>3.1</b>	<b>Total Field Magnetic Data</b> .....	<b>11</b>
<b>3.2</b>	<b>Radiometric data</b> .....	<b>13</b>
<b>4.</b>	<b>PRODUCTS</b> .....	<b>17</b>
<b>5.</b>	<b>REFERENCES</b> .....	<b>18</b>
	<b>APPENDIX A1: FLOW CHART OF MAGNETIC PROCESSING</b> .....	<b>19</b>
	<b>APPENDIX A2: DESCRIPTION OF THE MATLAB CODE</b> .....	<b>19</b>
	<b>APPENDIX A3: FLOW CHART OF RADIOMETRY PROCESSING</b> .....	<b>19</b>

## TABLES

<b>Table 1.</b>	<b>Flight specifications of the surveyed areas</b> .....	<b>5</b>
<b>Table 2.</b>	<b>Base station magnetometer locations (WGS-84, UTM-zone 32N)</b> .....	<b>7</b>
<b>Table 3.</b>	<b>Instrument Specifications</b> .....	<b>9</b>
<b>Table 4.</b>	<b>Survey Specifications Summary</b> .....	<b>9</b>
<b>Table 5.</b>	<b>Specified channel windows for the 1024 RSX-5 systems used in this survey</b> .....	<b>13</b>
<b>Table 6.</b>	<b>List of Geosoft XYZ files available from NGU on request.</b> .....	<b>17</b>
<b>Table 7.</b>	<b>Maps available from NGU on request.</b> .....	<b>17</b>

## FIGURES

<b>Figure 1: Kviteseid, Notodden and Ulefoss surveyed areas .....</b>	<b>5</b>
<b>Figure 2: Base station magnetometer locations .....</b>	<b>7</b>
<b>Figure 3: Base station magnetometer .....</b>	<b>8</b>
<b>Figure 4: Eurocopter AS350-B3 first helicopter used in survey .....</b>	<b>10</b>
<b>Figure 5: Pilots in front of the second helicopter used in survey .....</b>	<b>10</b>
<b>Figure 6: An example of Gamma-ray spectrum.....</b>	<b>13</b>
<b>Figure 7: Total Magnetic Field anomaly Kviteseid-Notodden-Ulefoss .....</b>	<b>21</b>
<b>Figure 8: Magnetic Vertical Gradient Kviteseid-Notodden-Ulefoss .....</b>	<b>22</b>
<b>Figure 9: Magnetic Horizontal Gradient Kviteseid-Notodden-Ulefoss.....</b>	<b>23</b>
<b>Figure 10: Magnetic Tilt Derivative Kviteseid-Notodden-Ulefoss.....</b>	<b>24</b>
<b>Figure 11: Uranium Ground Concentration Kviteseid-Notodden-Ulefoss .....</b>	<b>25</b>
<b>Figure 12: Thorium Ground Concentration Kviteseid-Notodden-Ulefoss .....</b>	<b>26</b>
<b>Figure 13: Potassium Ground Concentration Kviteseid-Notodden-Ulefoss.....</b>	<b>27</b>
<b>Figure 14: Ternary Image of Radiation Concentrations Kviteseid-Notodden-Ulefoss ...</b>	<b>28</b>

## 1. INTRODUCTION

Recognising the impact that investment in mineral exploration and mining can have on the socio-economic situation of a region, the government of Norway initiated the MINS program (Mineral resources in South Norway). The goal of this program is to enhance the geological information that is relevant to an assessment of the mineral potential of the three northernmost counties. The airborne geophysical surveys - helicopter borne and fixed wing- are important integral parts of MINS program. The airborne survey results reported herein amount about 9960 line km (1960 km<sup>2</sup>) over the surveyed areas, as shown in Figure 1.

The survey was divided into two phases during the acquisition period. The first phase started on June 4<sup>th</sup> 2013 and ended on July 5<sup>th</sup> 2013. During this phase more than 95% of the total measurements were done following the flight paths shown with blue in Figure 1. The areas over the two lakes, shown with red polygons in Figure 1., were not measured in this phase due to flying security restrictions. These areas were flown at a second phase by another helicopter-borne system by continuing the flight paths of the first phase (red lines in Fig. 1).

**Table 1. Flight specifications of the surveyed areas**

Phase	Area	Surveyed lines (km)	Surveyed area (Km <sup>2</sup> )	Flight direction	Average flight speed (km/h)
<b>A</b>	Kviteseid, Notodden and Ulefoss	9570	1860	NW-SE	80
<b>B</b>	<b>B1.</b> Norsjo and <b>B2.</b> Seljordsvatn	390	100	NW-SE	80
<b>Total</b>		<b>9960</b>	<b>1960</b>		

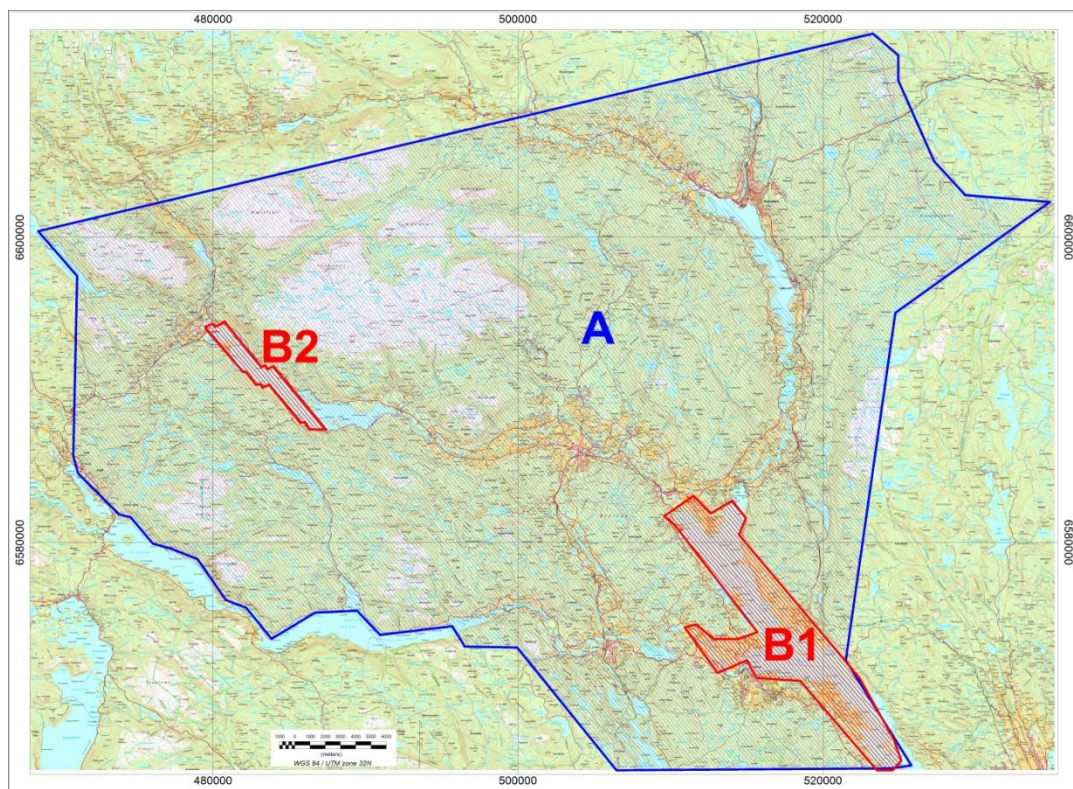


**Figure 1: A. Kviteseid, Notodden and Ulefoss surveyed areas. The blue lines mark the flight paths flown between June-July 2013. B1 Norsjo and B2 Seljordsvatn lakes shown with the red polygons. The red lines in these polygons mark the flight paths flown on 18th of October 2013.**

The objective of the airborne geophysical survey was to obtain a dense high-resolution aeromagnetic and radiometric data set over the survey area. These data sets are required for the enhancement of a general understanding of the regional geology of the area. In this regard, the data can also be used to map contacts and structural features within the area. It also improves defining the potential of known zones of mineralization, their geological settings, and identifying new areas of interest.

The survey incorporated the use of high-sensitivity Cesium magnetometers, gamma-ray spectrometers and radar altimeters. GPS navigation computer systems with flight path indicators ensured accurate positioning of the geophysical data with respect to the World Geodetic System 1984 geodetic datum (WGS-84).

## 2. SURVEY SPECIFICATIONS

### 2.1 Airborne Survey Parameters

NGU used two helicopter-borne systems for the purposes of this survey.

The *first system* (fig. 4) had a optically pumped Cesium magnetometer (Cs-2) towed 30 meter below the helicopter for the magnetic field recordings and a 1024 channel RSX-5 gamma-ray spectrometer fixed under the belly of the helicopter to map ground concentrations of Uranium, Thorium and Potassium. This system was used at the second phase of the survey to fill the gaps over the two lakes (B1 and B2 in fig 1.), and is described in more details in other NGU reports (i.e NGU Report 2013.047).

The *second system* (fig. 5), that conducted more than 95% of the measurements in this survey, is a helicopter-borne system that was designed to obtain detailed airborne magnetic and radiometric data. This system used a Scintrex Cs-3 housed in a 2 m long bird, towed 15 meters below the helicopter for the magnetic field recordings and a similar 1024 channel gamma-ray spectrometer to the one that was installed on the *first system*, to map ground concentrations of Uranium, Thorium and Potassium.

The first phase of the airborne survey began on June 4<sup>th</sup> and ended on July 05<sup>th</sup>, 2013. A Eurocopter AS350-B2 from the helicopter company HeliScan AS was used on this stage. The survey lines were spaced 200 m apart and the flight direction was NW-SE throughout the survey. Instrument operation was performed by HeliScan AS employees.

The second phase was conducted on 18<sup>th</sup> of October, 2013. A Eurocopter AS350-B3 helicopter from the same company with additional floats attached on its landing skids to overcome the flying restrictions over large water bodies was used to fly over the lakes.

Large water bodies, rugged terrain and abrupt changes in topography affected the pilot's ability to 'drape' the terrain; therefore there are positive and negative variations in sensor height with respect to the standard helicopter height, which is defined as 60 m plus a height of obstacles (trees, power lines). The average survey height for the magnetometer was about 50m for the *first system* and about 65 m for the *second system*, while for the spectrometer was at about 80m for both. Due to flight safety rules, especially over water bodies, parts of some profiles were flown at high altitudes. These data were discarded during the radiometric processing.

The ground speed of the aircraft varied from 60 – 120 km/h depending on topography, wind direction and its magnitude. On average the ground speed during the whole survey was about 80 km/h. The ground speeds for each sub-region are given in Table 1.

Magnetic data were recorded at 0.2 second intervals resulting in approximately 4.5 m point spacing. Spectrometry data was recorded every 1 second giving a point spacing of approximately 22 meters.

The above parameters were designed to allow for sufficient detail in the data to detect subtle anomalies that may represent mineralization and/or rocks of different lithological and petro-physical composition.

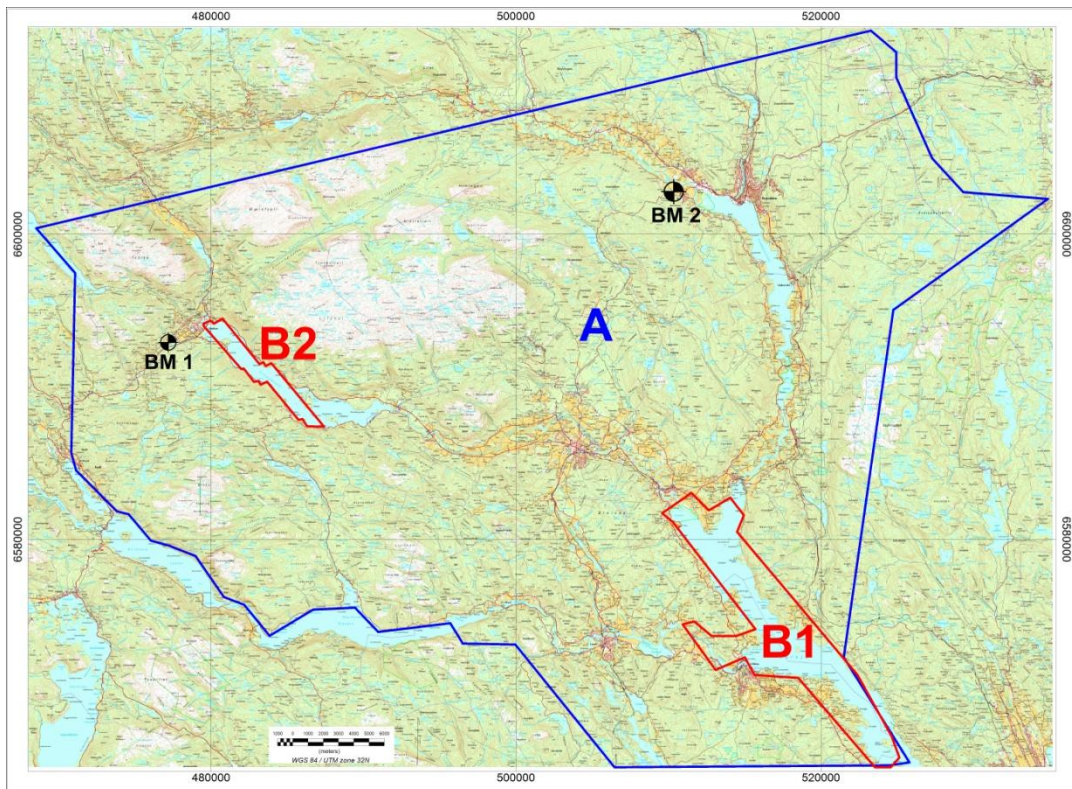


**Figure 2: Base station magnetometer locations**

A base magnetometer to monitor diurnal variations in the magnetic field, was installed close to the helicopter base during the whole survey period. The proximity to the areas under investigation impose changes to the helicopter base location, and therefore changes to the base magnetometer locations which are depicted on figure 2. Names and locations of the base magnetometer stations are given in Table 2.

**Table 2. Base station magnetometer locations (WGS-84, UTM-zone 32N)**

Base mag name	Location	UTM E (m)	UTM N (m)	Instrument	Sampling interval (sec)
<b>BM1</b>	Seljord	477200	6592900	Scintrex EnviMag	3
<b>BM2</b>	Notodden	510400	6602800	Scintrex EnviMag GEM GSM-19	3 10

A Scintrex EnviMag base station magnetometer was used to record data every 3 seconds for the first part of the survey (04/06 – 03/07), and was later accompanied by a GEM GSM-19 base magnetometer (26/06 – 05/07 and also on 18/10). The CPU clock of the magnetometers

was synchronized through the built-in GPS receiver to permit subsequent removal of diurnal drift. In order to bring the data from different base stations to the same level, complete recordings from the Dombås Observatory (505750E, 6882000N), Karmøy Observatory (285400E, 6569500N), and Solund Observatory (275700E, 6778800N), for the whole period of the survey, were used as reference. The variations in the recorded magnetic field at the base stations were similar to those recorded at the magnetic observatory of Dombås, which lies about 280 km north of the surveyed area, and therefore the continuous recordings from that observatory were used to level the magnetic base station data.



**Figure 3: A base station magnetometer (GEM GSM-19) installed 4 km northwest of Notodden**

Navigation system uses GPS/GLONASS satellite tracking systems to provide real-time WGS-84 coordinate locations for every second. The accuracy achieved with no differential corrections is reported to be  $\pm 5$  m in the horizontal directions. The GPS receiver antenna was mounted externally to the tail tip of the helicopter.

For quality control, the magnetic, radiometric, altitude and navigation data were monitored on two separate windows in the operator's display during flight while they were recorded in ASCII data streams to the acquisition PC hard disk drive.

## 2.2 Airborne Survey Instrumentation

Instrument specifications are given in table 3.

**Table 3. Instrument Specifications**

Instrument	Producer/Model	Accuracy / Sensitivity	Sampling frequency / interval
Magnetometer	Scintrex Cs-3	<2.5 nT	5 Hz
	Scintrex Cs-2	<2.5 nT	5 Hz
Base magnetometer	Scintrex EnviMag	0.1 nT	3 s
	GEM GSM-19	0.1 nT	10 s
Gamma spectrometer	Radiation Solutions RSX-5	1024 ch's, 16 liters down, 4 liters up	1 Hz
Radar altimeter	Bendix/King KRA 405B	± 3 % 0 – 500 feet ± 5 % 500 – 2500 feet	1 Hz
Pressure/temperature	Honeywell PPT	± 0.03 % FS	1 Hz
Navigation	Topcon GPS-receiver	± 5 meter	1 Hz
Acquisition system	NGU custom software		

The magnetic and radiometric, altitude and navigation data were monitored on the operator's displays during flight while they were recorded to the PC hard disk drive. Spectrometry data were also recorded to internal hard drive of the spectrometer. The data files were transferred to the field workstation via USB flash drive. The raw data files were backed up onto USB flash drive in the field.

## 2.3 Airborne Survey Logistics Summary

A summary of the survey specifications is shown in Table 4.

**Table 4. Survey Specifications Summary**

Parameter	Specifications
Traverse (survey) line spacing	200 metres
Traverse line direction	NW-SE
Nominal aircraft ground speed	60 - 120 km/h
Average sensor terrain clearance Mag	50m (first system) 65m (second system)
Average sensor terrain clearance Rad	80m (first system) 80m (second system)
<b>Sampling rates:</b>	
Magnetometer	0.2 seconds
Spectrometer, GPS, altimeter	1.0 second



**Figure 4: The Eurocopter AS350-B3 with the additional floats attached to its landing skids, that was used to conduct measurements over the lakes.**



**Figure 5: Pilots Småland and Lorentzen with Mag bird in front of the second helicopter used in survey. (P1)**

### 3. DATA PROCESSING AND PRESENTATION

All data were processed by Alexandros Stampolidis at NGU. The ASCII data files for each phase were loaded into separate Oasis Montaj databases. The datasets were processed consequently according to processing flow charts shown in Appendix A1 and A3.

#### 3.1 Total Field Magnetic Data

At the first stage the raw magnetic data of each phase of data acquisition were stored in two different databases and checked for spikes, using the 4th difference calculation as a flag. Obvious spikes were checked and then manually removed. The data from base stations were also inspected for spikes and spikes were removed manually if necessary. Typically, several corrections have to be applied to magnetic data before gridding – i.e. heading, lag and diurnal correction.

##### Special magnetic processing problems

The small wing area of the bird and the relative low flight speed during parts of the survey, caused the bird to swing with a pendulum effect. The 15 m rope gave this pendulum motion a period of about 7.5 seconds. The effect of the swinging motion was clearly visible in the magnetic data and made it necessary to apply a special filter in order to reduce the noise that was prominent in parts of the survey. This was achieved using a Matlab code developed by Alexandros Stampolidis (see description on Appendix A2). This step was applied before the diurnal corrections.

##### Diurnal Corrections

The temporal fluctuations in the magnetic field of the earth affect the total magnetic field readings during the airborne survey. This is commonly referred to as the magnetic diurnal variation. These fluctuations can be effectively removed from the airborne magnetic dataset by using a stationary reference magnetometer that records the magnetic field of the earth at a given short time interval. Magnetic diurnals that were recorded on the base station magnetometers, were within the standard NGU specifications during the entire survey (Rønning 2013).

Between 04/6 to 03/7 diurnal variations were measured with a Scintrex Envimag base station magnetometer, while from 26/6 to 05/7 and also on 18/10, a GEM GSM-19 magnetometer was employed. The base station computer clock was continuously synchronized with GPS clock. The recorded data are merged with the airborne data and the diurnal correction is applied according to equation (1).

$$\mathbf{B}_{Tc} = \mathbf{B}_T + (\bar{B}_B - \mathbf{B}_B), \quad (1)$$

Where:

$\mathbf{B}_{Tc}$  = Corrected airborne total field readings

$\mathbf{B}_T$  = Airborne total field readings

$\bar{B}_B$  = Average datum base level

$\mathbf{B}_B$  = Base station readings

The average datum base level ( $\bar{B}_B$ ) was set equal to 50566.7 nT for the first phase of survey (blue flight paths on Fig.1), and equal to 50536.9 nT for the second phase (red flight paths on Fig.1) allowing us to bring recorded magnetic data of the entire survey to a common level.

### Corrections for Lag and heading

Neither a lag nor cloverleaf tests were performed before the survey. According to previous reports the lag between logged magnetic data and the corresponding navigational data was 1-2 fids. Translated to a distance it would be no more than 10 m - the value comparable with the precision of GPS. A heading error for a towed system is usually either very small or non-existent. So no lag and heading corrections were applied.

### Magnetic data processing, gridding and presentation

The total field magnetic anomaly data ( $\mathbf{B}_{TA}$ ) were calculated from the diurnal corrected data ( $\mathbf{B}_{Tc}$ ) after subtracting the IGRF for the surveyed area calculated for the data period (eq.2)

$$\mathbf{B}_{TA} = \mathbf{B}_{Tc} - IGRF \quad (2)$$

The total field anomaly data ( $\mathbf{B}_{TA}$ ) of each phase were joined in a common database, split in lines and then were gridded using a minimum curvature method with a grid cell size of 50 meters. This cell size is equal to one quarter of the 200m average line spacing. In order to remove small line-to-line levelling errors that were detected on the gridded magnetic anomaly data, the Geosoft Micro-levelling technique was applied on the flight line based magnetic database. Then, the micro-levelled channel was gridded using again a minimum curvature method with 50 m grid cell size.

The processing steps of magnetic data presented so far were performed on point basis. The following steps are performed on grid basis. The Horizontal and Vertical Gradient along with the Tilt Derivative of the total magnetic anomaly were calculated from the micro-levelled total magnetic anomaly grid. The magnitude of the horizontal gradient was calculated according to equation (3)

$$HG = \sqrt{\left(\frac{\partial(B_{TA})}{\partial x}\right)^2 + \left(\frac{\partial(B_{TA})}{\partial y}\right)^2} \quad (3)$$

where  $\mathbf{B}_{TA}$  is the micro-levelled field. The vertical gradient (VG) was calculated by applying a vertical derivative convolution filter to the micro-levelled  $\mathbf{B}_{TA}$  field. The Tilt derivative or Tilt angle (TD) was calculated according to the equation (4)

$$TD = \tan^{-1}\left(\frac{VG}{HG}\right) \quad (4)$$

The last step in the magnetic data processing involved a low pass Fourier filter applied on the gridded micro-levelled data. The cutoff wavelength was set equal to 300m (LP300). The gradients and Tilt derivative were recalculated setting LP300 as input grid in the calculations.

The results are presented in series of coloured shaded relief maps at scale of 1:75000. These maps are:

- A. Total field magnetic anomaly
- B. Horizontal gradient of total magnetic anomaly
- C. Vertical gradient of total magnetic anomaly
- D. Tilt Derivative (or Tilt angle) of the total magnetic anomaly

and they are representative of the distribution of magnetization over the surveyed areas. A list of the produced maps is shown on Table 7.

### 3.2 Radiometric data

Airborne gamma-ray spectrometry measures the abundance of Potassium (K), Thorium (eTh), and Uranium (eU) in rocks and weathered materials by detecting gamma-rays emitted due to the natural radioelement decay of these elements. The data analysis method is based on the IAEA recommended method for U, Th and K (International Atomic Energy Agency, 1991; 2003). A short description of the individual processing steps of that methodology as adopted by NGU is given below:

#### Energy windows

The Gamma-ray spectra were initially reduced into standard energy windows corresponding to the individual radio-nuclides K, U and Th. Figure 6 shows an example of a Gamma-ray spectrum and the corresponding energy windows and radioisotopes (with peak energy in MeV) responsible for the radiation.

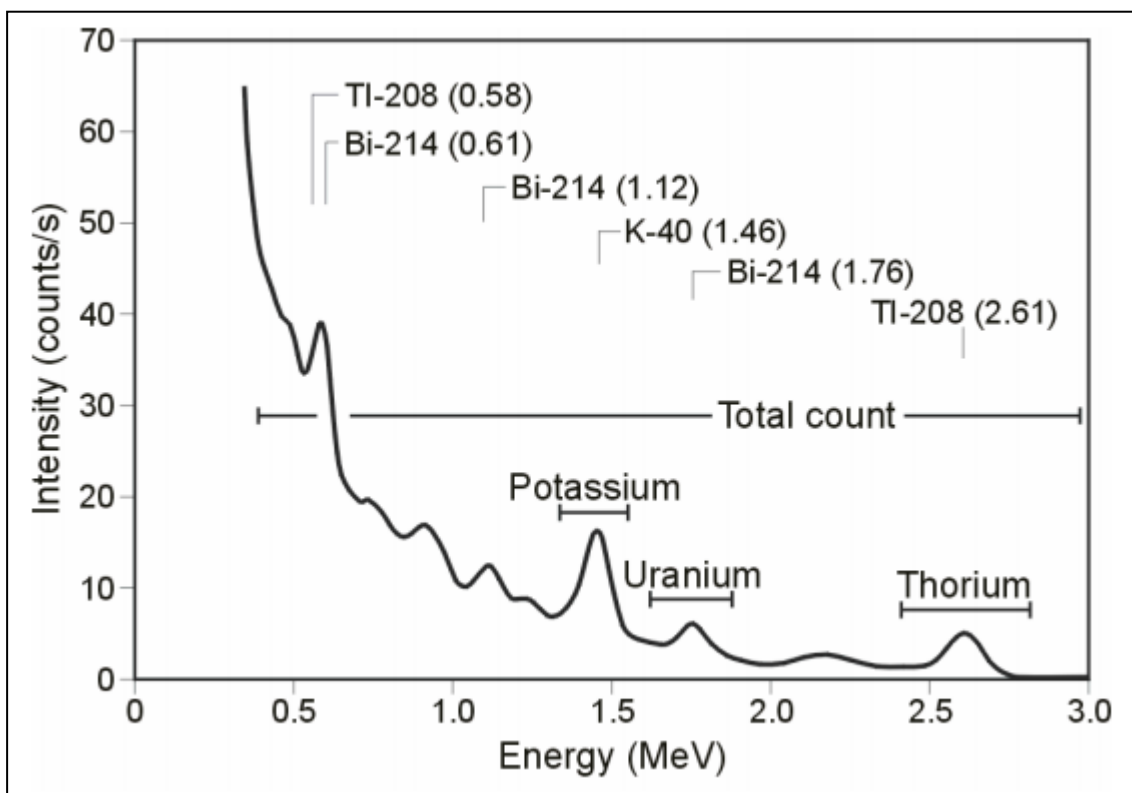


Figure 6: An example of Gamma-ray spectrum showing the position of the K, Th, U and Total count windows.

Table 5. Specified channel windows for the 1024 RSX-5 systems used in this survey

Gamma-ray spectrum	Cosmic	Total count	K	U	Th
Down	1022	134-934	454-521	551-617	801-934
Up	1022			551-617	
Energy windows (MeV)	>3.07	0.41-2.81	1.37-1.57	1.66-1.859	2.41-2.81

The RSX-5 is a 1024 channel system with four downward and one upward looking detectors, which means that the actual Gamma-ray spectrum is divided into 1024 channels. The first channel is reserved for the “Live Time” and the last for the Cosmic rays. Table 5 shows the channels that were used for the reduction of the spectrum.

### Live Time correction

The data were corrected for live time. “Live time” is an expression of the relative period of time the instrument was able to register new pulses per sample interval. On the other hand “dead time” is an expression of the relative period of time the system was unable to register new pulses per sample interval. The relation between “dead” and “live time” is given by the equation (5)

$$\text{“Live time”} = \text{“Real time”} - \text{“Dead time”} \quad (5)$$

where the “real time” or “acquisition time” is the elapsed time over which the spectrum is accumulated (1 second).

The live time correction is applied to the total count, Potassium, Uranium, Thorium, upward Uranium and cosmic channels. The formula used to apply the correction is as follows:

$$C_{LT} = C_{RAW} \cdot \frac{1000000}{Live\ Time} \quad (6)$$

where  $C_{LT}$  is the live time corrected channel in counts per second,  $C_{RAW}$  is the raw channel data in counts per second and Live Time is in microseconds.

### Cosmic and aircraft correction

Background radiation resulting from cosmic rays and aircraft contamination was removed from the total count, Potassium, Uranium, Thorium, upward Uranium channels using the following formula:

$$C_{CA} = C_{LT} - (a_c + b_c \cdot C_{Cos}) \quad (7)$$

where  $C_{CA}$  is the cosmic and aircraft corrected channel,  $C_{LT}$  is the live time corrected channel  $a_c$  is the aircraft background for this channel,  $b_c$  is the cosmic stripping coefficient for this channel and  $C_{Cos}$  is the low pass filtered cosmic channel.

### Radon correction

The upward detector method, as discussed in IAEA (1991), was applied to remove the effects of the atmospheric radon in the air below and around the helicopter. Usages of over-water measurements where there is no contribution from the ground, enabled the calculation of the coefficients ( $a_C$  and  $b_C$ ) of the linear equations that relate the cosmic corrected counts per second of Uranium channel with total count, Potassium, Thorium and Uranium upward channels over water. Data over-land was used in conjunction with data over-water to calculate the  $a_1$  and  $a_2$  coefficients used in equation (8) for the determination of the Radon component in the downward uranium window:

$$Radon_U = \frac{U_{upCA} - a_1 \cdot U_{CA} - a_2 \cdot Th_{CA} + a_2 \cdot b_{Th} - b_U}{a_U - a_1 - a_2 \cdot a_{Th}} \quad (8)$$

where  $Radon_u$  is the radon component in the downward uranium window,  $U_{upCA}$  is the filtered upward uranium,  $U_{CA}$  is the filtered Uranium,  $Th_{CA}$  is the filtered Thorium,  $a_1$ ,  $a_2$ ,  $a_U$  and  $a_{Th}$  are proportional factors and  $b_U$  and  $b_{Th}$  are constants determined experimentally.

The effects of Radon in the downward Uranium are removed by simply subtracting  $Radon_U$  from  $U_{CA}$ . The effects of radon in the other channels are removed using the following formula:

$$C_{RC} = C_{CA} - (a_C \cdot Radon_U + b_C) \quad (9)$$

where  $C_{RC}$  is the Radon corrected channel,  $C_{CA}$  is the cosmic and aircraft corrected channel,  $Radon_U$  is the Radon component in the downward uranium window,  $a_C$  is the proportionality factor and  $b_C$  is the constant determined experimentally for this channel from over-water data.

### Compton Stripping

Potassium, Uranium and Thorium Radon corrected channels, are subjected to spectral overlap correction. Compton scattered gamma rays in the radio-nuclides energy windows were corrected by window stripping using Compton stripping coefficients determined from measurements on calibration pads at the Geological Survey of Norway in Trondheim (for values, see Appendix A3).

The stripping corrections are given by the following formulas:

$$A_1 = 1 - (g \cdot \gamma) - (a \cdot \alpha) + (a \cdot g \cdot \beta) - (b \cdot \beta) + (b \cdot \alpha \cdot \gamma) \quad (10)$$

$$U_{ST} = \frac{Th_{RC} \cdot ((g \cdot \beta) - \alpha) + U_{RC} \cdot (1 - b \cdot \beta) + K_{RC} \cdot ((b \cdot \alpha) - g)}{A_1} \quad (11)$$

$$Th_{ST} = \frac{Th_{RC} \cdot (1 - (g \cdot \gamma)) + U_{RC} \cdot (b \cdot \gamma - a) + K_{RC} \cdot ((a \cdot g) - b)}{A_1} \quad (12)$$

$$K_{ST} = \frac{Th_{RC} \cdot ((\alpha \cdot \gamma) - \beta) + U_{RC} \cdot ((a \cdot \beta) - \gamma) + K_{RC} \cdot (1 - (a \cdot \alpha))}{A_1} \quad (13)$$

where  $U_{RC}$ ,  $Th_{RC}$ ,  $K_{RC}$  are the radon corrected Uranium, Thorium and Potassium and  $a$ ,  $b$ ,  $g$ ,  $\alpha$ ,  $\beta$ ,  $\gamma$  are Compton stripping coefficients.

### Reduction to Standard Temperature and Pressure

The radar altimeter data were converted to effective height ( $H_{STP}$ ) using the acquired temperature and pressure data, according to the expression:

$$H_{STP} = H \cdot \frac{273.15}{T + 273.15} \cdot \frac{P}{1013.25} \quad (14)$$

where  $H$  is the smoothed observed radar altitude in meters,  $T$  is the measured air temperature in degrees Celsius and  $P$  is the measured barometric pressure in millibars.

### Height correction

Variations caused by changes in the aircraft altitude relative to the ground was corrected to a nominal height of 60 m. Data recorded at the height above 150 m were considered as non-reliable and removed from processing. Total count, Uranium, Thorium and Potassium stripped channels were subjected to height correction according to the equation:

$$C_{60m} = C_{ST} \cdot e^{C_{ht}(60-H_{STP})} \quad (15)$$

where  $C_{ST}$  is the stripped corrected channel,  $C_{ht}$  is the height attenuation factor for that channel and  $H_{STP}$  is the effective height.

### Conversion to ground concentrations

Finally, corrected count rates were converted to effective ground element concentrations using calibration values derived from calibration pads at the Geological Survey of Norway in Trondheim (for values, see Appendix A3). The corrected data provide an estimate of the apparent surface concentrations of Potassium, Uranium and Thorium ( $K$ ,  $eU$  and  $eTh$ ). Potassium concentration is expressed as a percentage, equivalent Uranium and Thorium as parts per million. Uranium and Thorium are described as “equivalent” since their presence is inferred from gamma-ray radiation from daughter elements ( $^{214}\text{Bi}$  for Uranium,  $^{208}\text{Tl}$  for Thorium).

The concentrations of each element is calculated according to the following expression:

$$C_{CONC} = C_{60m} / C_{SENS\_60m} \quad (16)$$

where  $C_{60m}$  is the height corrected channel,  $C_{SENS\_60m}$  is experimentally determined sensitivity reduced to the nominal height (60m).

#### **Spectrometry data gridding and presentation**

Gamma-rays from Potassium, Thorium and Uranium emanate from the uppermost 30 to 40 centimetres of soil and rock in the crust (Minty, 1997). Variations in the concentrations of these radioelements largely related to changes in the mineralogy and geochemistry of the Earth's surface.

The spectrometry data were stored in two databases, one for each phase, and the ground concentrations were calculated following the processing steps. A list of the parameters used in these steps, for each phase, is given in Appendix A3.

Subsequently, the two databases were joined into a single database, split in lines and then ground concentrations of the three main natural radio-elements Potassium, Thorium and Uranium and total gamma-ray flux (total count) were gridded using a minimum curvature method with a grid cell size of 50 meters. In order to remove small line-to-line levelling errors appeared on those grids, the data were micro-levelled as in the case of the magnetic data, and re-gridded with the same grid cell size. Finally, a 3x3 convolution filter was applied to smooth the microlevelled grids. A list of the produced maps is shown on Table 7.

Quality of the radiometric data was within standard NGU specifications (Rønning 2013). For further reading regarding standard processing of airborne radiometric data, we recommend the publications from Minty et al. (1997).

#### 4. PRODUCTS

Processed digital data from the survey are presented as:

1. Geosoft XYZ files as show in table 6:

**Table 6. List of Geosoft XYZ files available from NGU on request.**

Name	Mag	Rad
Kviteseid-Notodden-Ulefoss	√	√

2. Georeferenced tiff files (Geo-tiff).
3. Coloured maps (jpg) at the scale 1:75.000 available from NGU on request (see Table 7.).

**Table 7. Maps available from NGU on request.**

Region	Map #	Scale	Name
Kviteseid- Notodden- Ulefoss	2013.049-01	1:75.000	Total filed magnetic anomaly
	2013.049-02	1:75.000	Magnetic Vertical Derivative
	2013.049-03	1:75.000	Magnetic Horizontal Derivative
	2013.049-04	1:75.000	Magnetic Tilt Derivative
	2013.049-05	1:75.000	Uranium ground concentration
	2013.049-06	1:75.000	Thorium ground concentration
	2013.049-07	1:75.000	Potassium ground concentration
	2013.049-08	1:75.000	Radiometric Ternary Map

Downscaled images of the maps are shown on figures 7 to 14.

## 5. REFERENCES

Geosoft 2010: Montaj MAGMAP Filtering, 2D-Frequency Domain Processing of Potential Field Data, Extension for Oasis Montaj v 7.1, Geosoft Corporation

Geotech 1997: Hummingbird Electromagnetic System. User manual, Geotech Ltd, October 1997

Grasty, R.L., Holman, P.B. & Blanchard 1991: Transportable Calibration pads for ground and airborne Gamma-ray Spectrometers. Geological Survey of Canada, Paper 90-23: 62 pp.

IAEA 1991: Airborne Gamma-Ray Spectrometry Surveying, Technical Report No 323, Vienna, Austria, 97 pp.

IAEA 2003: Guidelines for radioelement mapping using gamma ray spectrometry data. IAEA-TECDOC-1363, Vienna, Austria, 173 pp.

Minty, B.R.S. 1997: The fundamentals of airborne gamma-ray spectrometry. AGSO Journal of Australian Geology and Geophysics, 17 (2): 39-50.

Minty, B.R.S., Luyendyk, A.P.J. and Brodie, R.C. 1997: Calibration and data processing for gamma-ray spectrometry. AGSO Journal of Australian Geology and Geophysics, 17(2): 51-62.

Naudy, H. and Dreyer, H. 1968: Non-linear filtering applied to aeromagnetic profiles. Geophysical Prospecting, 16(2): 171-178.

Rønning, J.S. 2013: NGUs helikoptermålinger. Plan for sikring og kontroll av datakvalitet. NGU Intern rapport 2013.001, (38 sider).

P1: Photo by Mari Nymoene, Telen Newspaper, Notodden

## APPENDIX A1: FLOW CHART OF MAGNETIC PROCESSING

Meaning of parameters is described in the referenced literature.

Processing flow:

- Quality control.
- Visual inspection of airborne data and manual spike removal
- Inspection of basemag data and removal of spikes
- Special Matlab convolution lowpass-filter for removal of 7.5 sec pendulum noise
- Import basemag data to Geosoft database
- Correction of data for diurnal variation and IGRF
- Splitting flight data by lines
- Gridding
- Micro-leveling
- USGS 2D-Frequency Domain filtering to remove high frequency noise and smooth data

## APPENDIX A2: DESCRIPTION OF THE MATLAB CODE

The code is being used to filter the “pendulum effect” periodic noise on the magnetic data. The data are filtered by calling a Matlab built-in convolution routine called “conv” that convolves the input data vector with a vector that has coefficients of Gaussian lowpass filter at a certain frequency (Freq.1).

If the differences between the input and the filtered data are above a predefined threshold, this part of the data is reprocessed by employing a less severe filter (Freq.2) on the input data. Again a threshold is applied on the differences between the input and the filtered data and in this case if the differences are above the threshold then the input data are retained for that part on the final filtered dataset.

These steps enable us to preserve the amplitudes of strong anomalies in the data, which will be lost otherwise by typical convolution or Fourier filtering. The cutoff frequency that were used were Freq.1=0.04Hz and Freq.2=0.09Hz.

## APPENDIX A3: FLOW CHART OF RADIOMETRY PROCESSING

Underlined processing stages are applied to the K, U, Th and TC windows.  
Meaning of parameters is described in the referenced literature.

Processing flow:

- Quality control
- Airborne and cosmic correction (IAEA, 2003)  
Used parameters: (determined by high altitude calibration flights near Langoya in July 2013 for the **first system** and at Frosta in May 2013 for the **second system**)

Channel	Aircraft background counts		Cosmic background counts	
	<i>first system</i>	<i>second system</i>	<i>first system</i>	<i>second system</i>
K	7.33	5.36	0.0617	0.0570
U	0.90	1.43	0.0454	0.0467
Th	0.89	0.00	0.0647	0.0643
Uup	0.39	0.70	0.0423	0.0448
Total counts	36.29	42.73	1.0379	1.0317

- Radon correction using upward detector method (IAEA, 2003)  
Used parameters (determined from survey data from both phases over water and land):

Coefficient	<i>first system</i>	<i>second system</i>	Coefficient	<i>first system</i>	<i>second system</i>
$a_u$	0.33302	0.18288	$b_u$	0.04641	0.0
$a_K$	1.03421	0.7263	$b_K$	0.00605	2.36856
$a_{Th}$	0.1086	0.23215	$b_{Th}$	0.0	0.63491
$a_{TC}$	15.6428	14.9534	$b_{TC}$	0.48734	14.2466
$a_1$	0.06367	0.063	$a_2$	0.02714	0.03478

- Stripping correction (IAEA, 2003)  
Used parameters (determined from measurements on calibrations pads at the NGU in May 2013):

Coefficient	<i>first system</i>	<i>second system</i>
a	0.049524	0.046856
b	0	0
c	0	0
$\alpha$	0.29698	0.30346
$\beta$	0.47138	0.47993
$\gamma$	0.82905	0.82316

- Height correction to a height of 60 m  
Used parameters (determined by high altitude calibration flights at Frosta in Jan 2014):  
Attenuation factors in 1/m:

Channel	<i>first system</i>	<i>second system</i>
K	-0.008884	-0.009523
U	-0.006528	-0.006687
Th	-0.006617	-0.007394
TC	-0.007331	-0.00773

- Converting counts at 60 m heights to element concentration on the ground  
Used parameters (determined from measurements on calibrations pads at the NGU in May 2013):  
Sensitivity (elements concentrations per count):

Channel	<i>first system</i>	<i>second system</i>
K (%/count)	0.007544793	0.007457884
U (ppm/count)	0.088909372	0.087729968
Th (ppm/count)	0.151433049	0.156658412

- Microlevelling using Geosoft menu and smoothening by a convolution filtering

Microlevelling parameters	<i>values</i>
De-corrugation cutoff wavelength (m)	2000
Cell size for gridding (m)	50
Naudy (1968) Filter length (m)	800

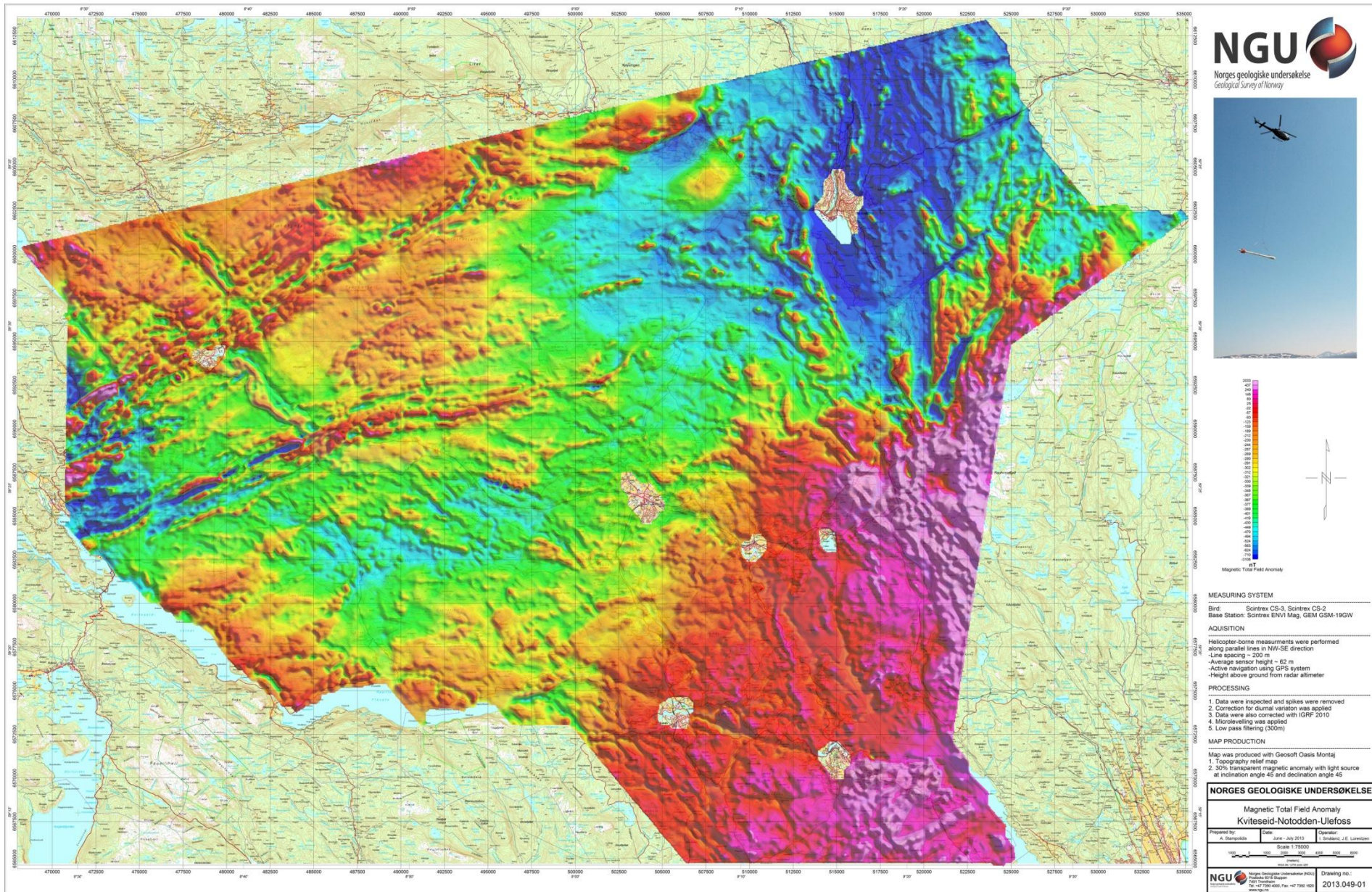


Figure 7: Total Magnetic Field anomaly Kviteseid-Notodden-Ulefoss

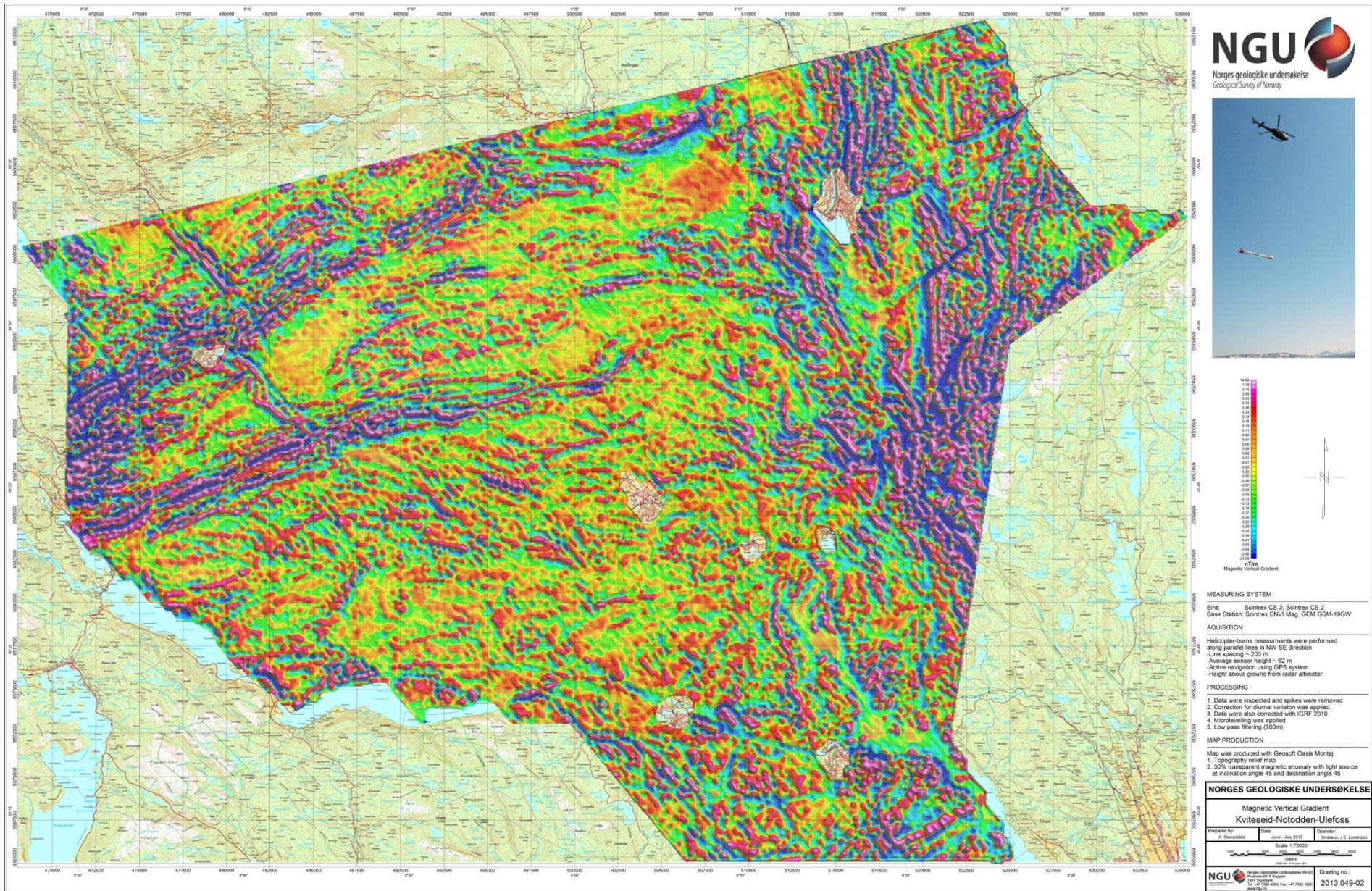


Figure 8: Magnetic Vertical Gradient Kviteseid-Notodden-Ulefoss

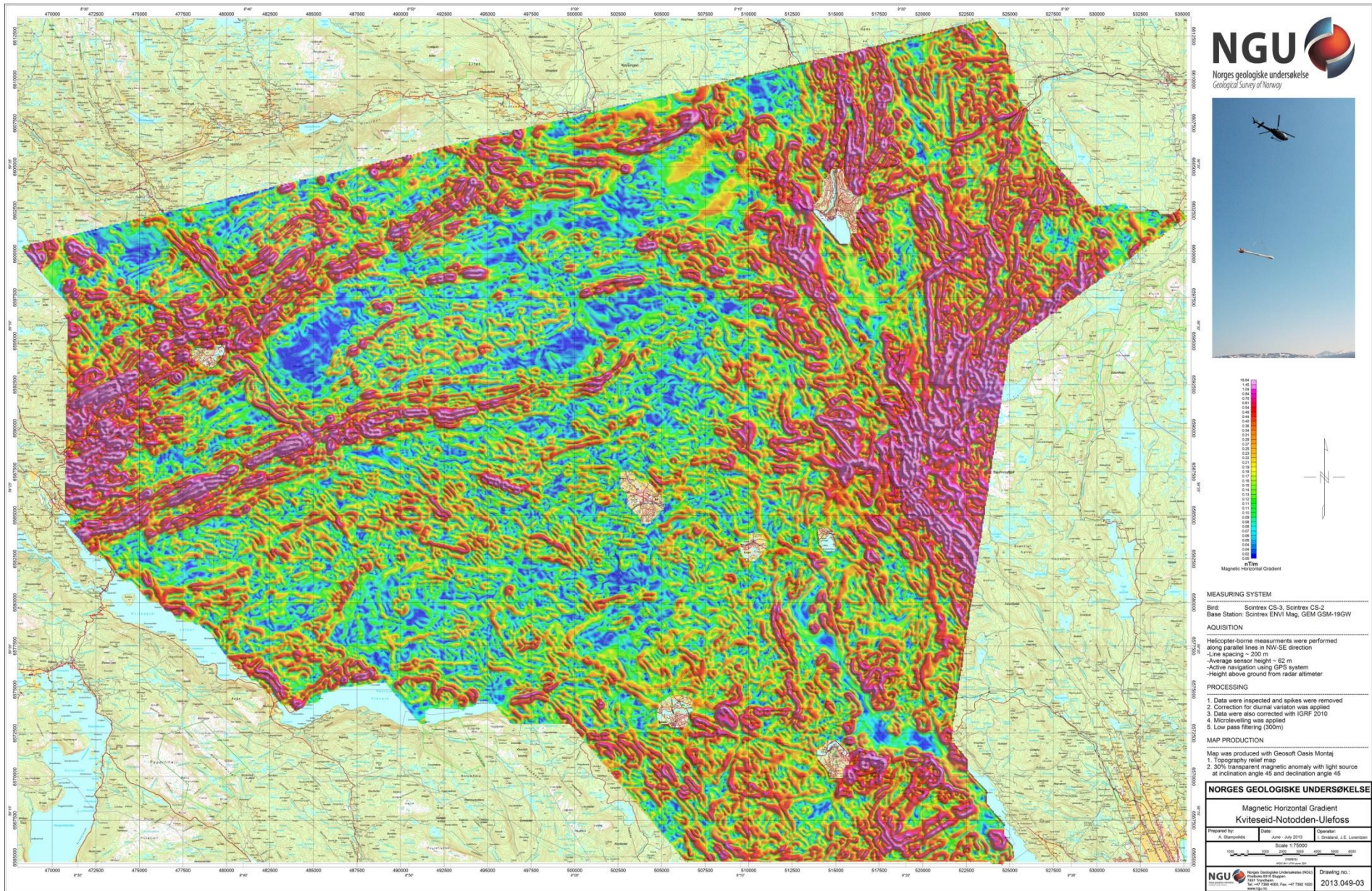


Figure 9: Magnetic Horizontal Gradient Kviteseid-Notodden-Ulefoss

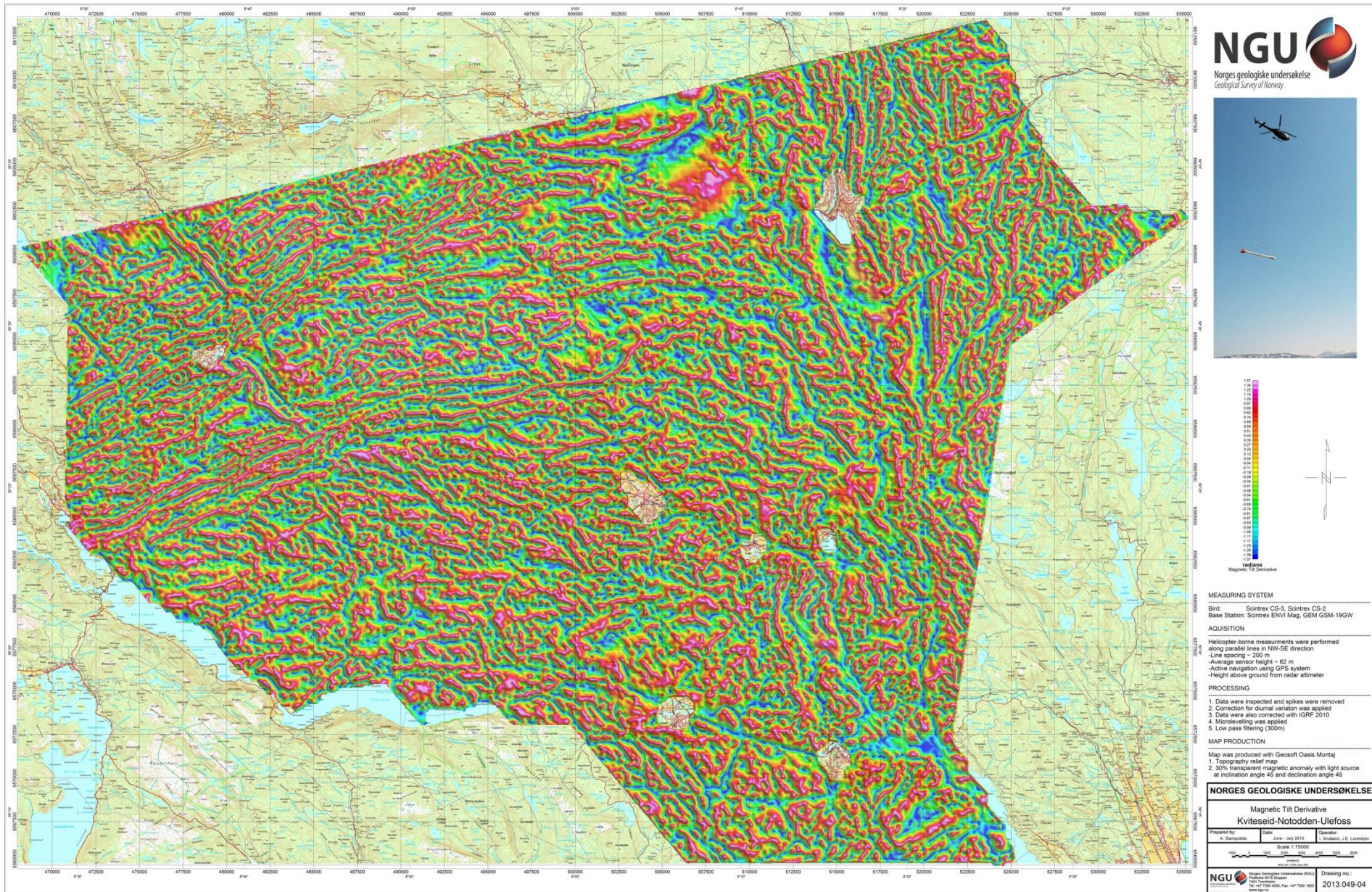


Figure 10: Magnetic Tilt Derivative Kviteseid-Notodden-Ulefoss

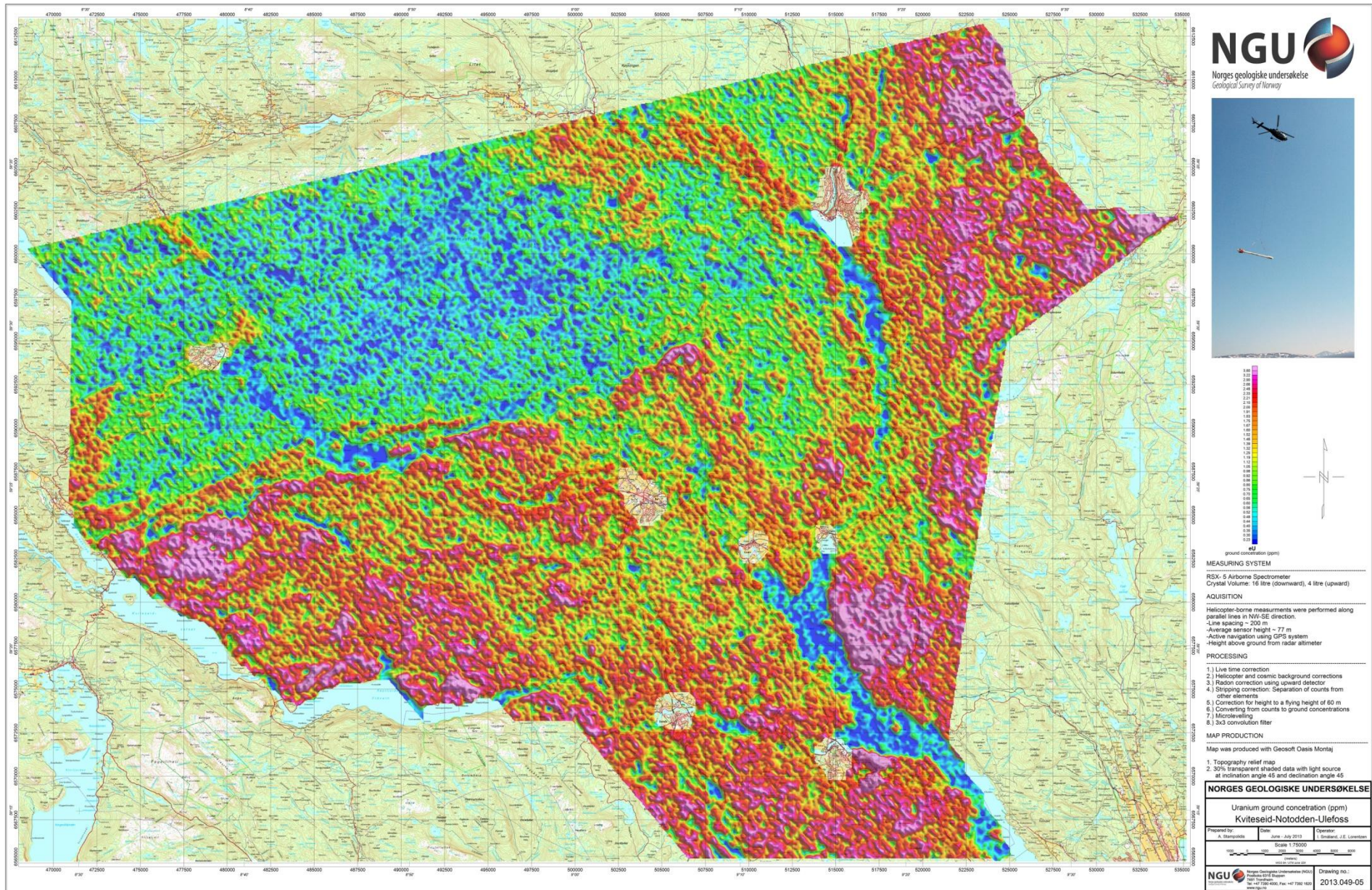


Figure 11: Uranium Ground Concentration Kviteseid-Notodden-Ulefoss

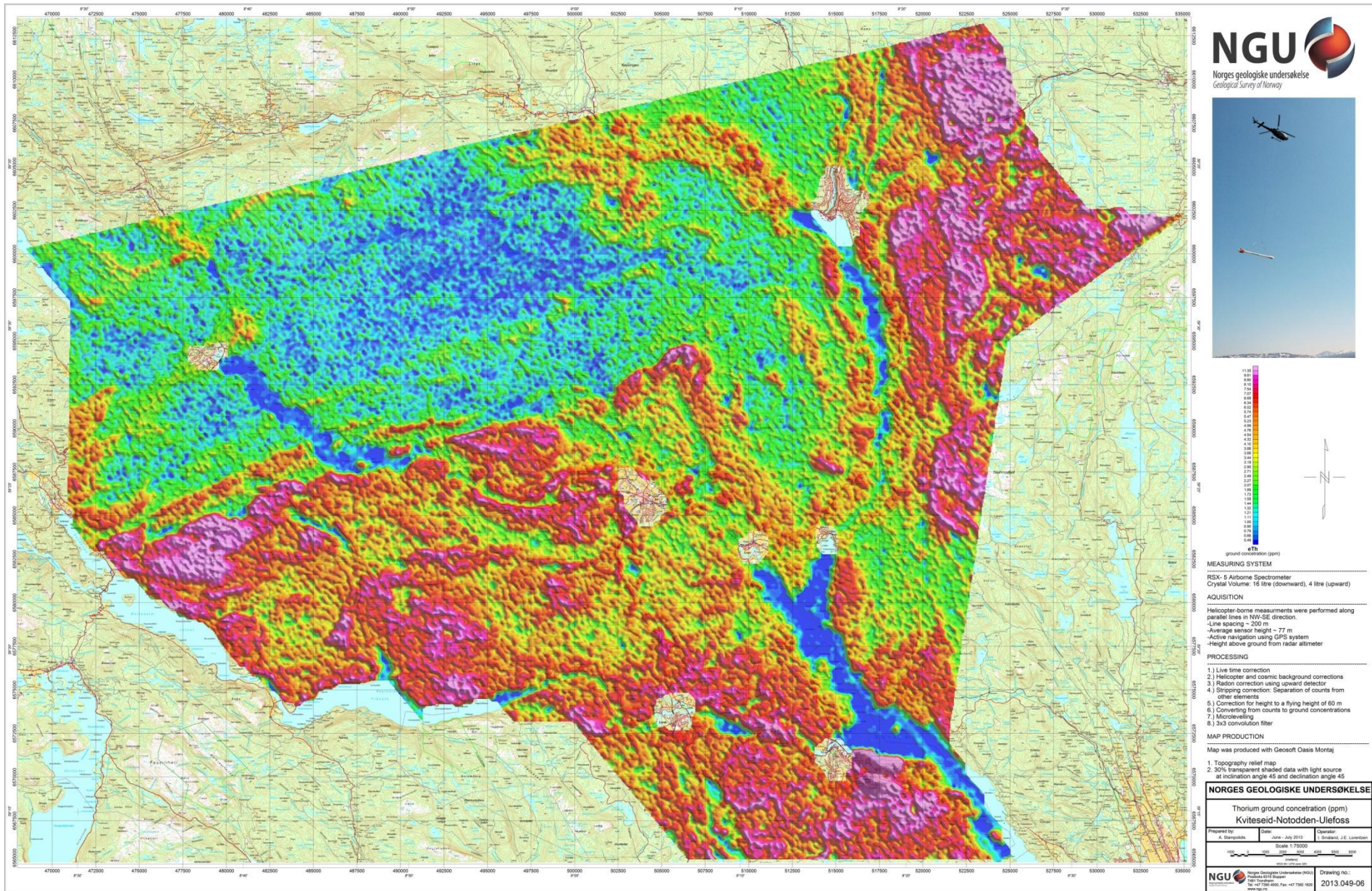


Figure 12: Thorium Ground Concentration Kviteseid-Notodden-Ulefoss

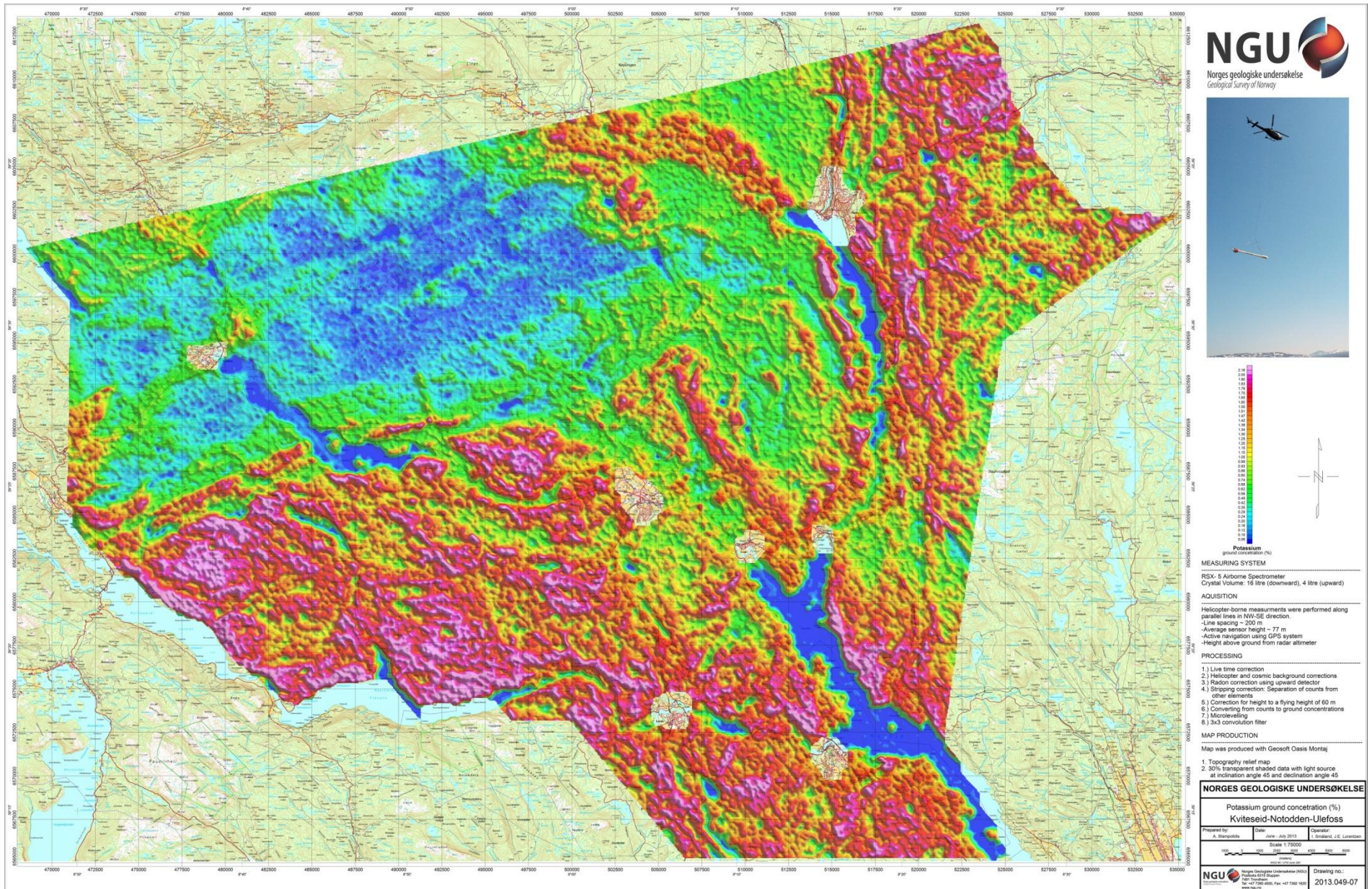


Figure 13: Potassium Ground Concentration Kviteseid-Notodden-Ulefoss

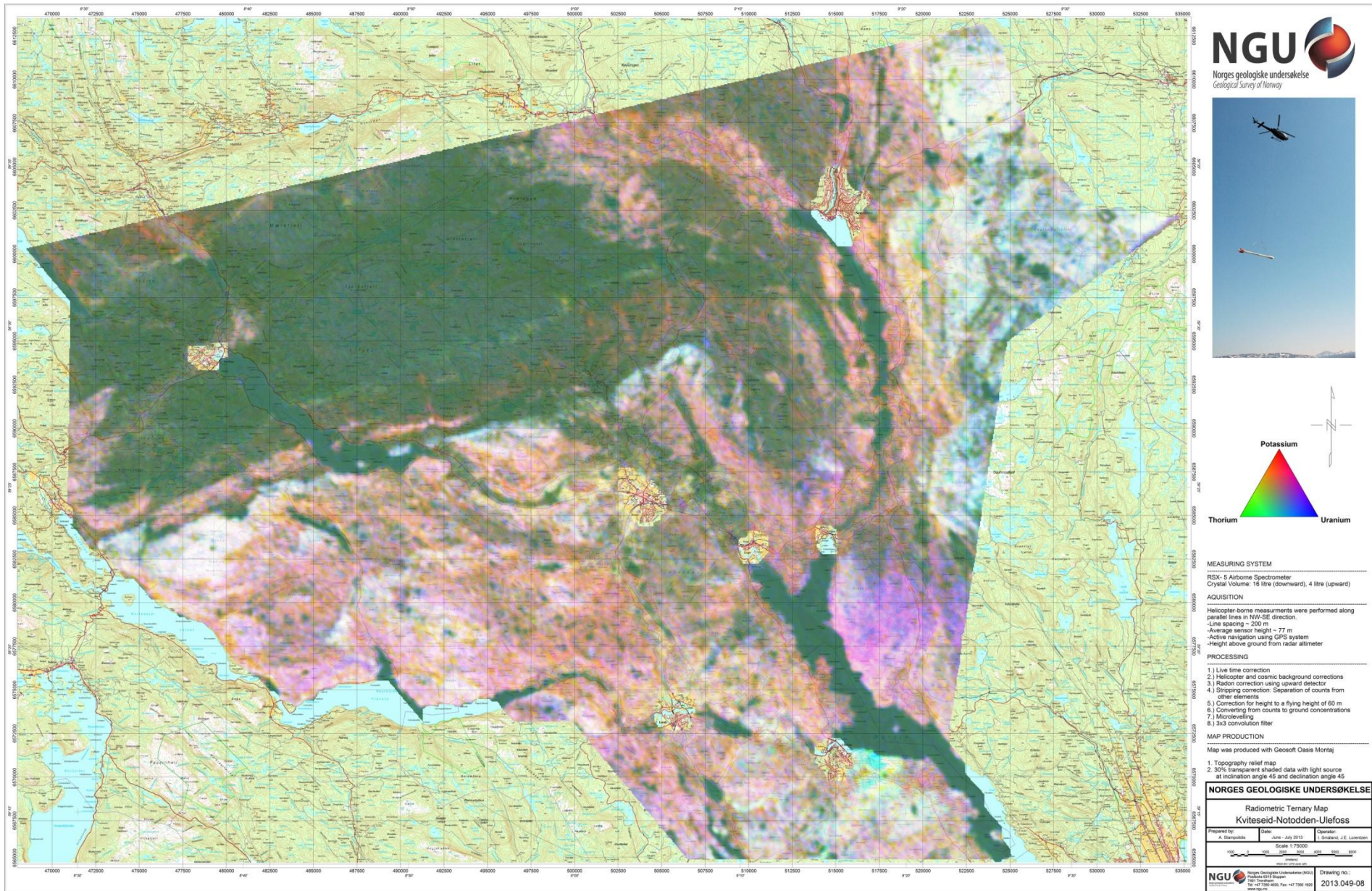


Figure 14: Ternary Image of Radiation Concentrations Kviteseid-Notodden-Ulefoss